Molecular Crystals and Liquid Crystals

ISSN: 1542-1406 (Print) 1563-5287 (Online) Journal homepage: http://www.tandfonline.com/loi/gmcl20

X-Ray Studies of Two Liquid Crystalline Compounds

M. K. Usha, N. Vinutha, R. Somashekar & D. Revannasiddaiah

To cite this article: M. K. Usha, N. Vinutha, R. Somashekar & D. Revannasiddaiah (2015) X-Ray Studies of Two Liquid Crystalline Compounds, Molecular Crystals and Liquid Crystals, 623:1, 9-16, DOI: 10.1080/15421406.2014.990749

To link to this article: http://dx.doi.org/10.1080/15421406.2014.990749

Mol. Cryst. Liq. Cryst., Vol. 623: pp. 9–16, 2015

ISSN: 1542-1406 print/1563-5287 online
DOI: 10.1080/15421406.2014.990749

Taylor & Francis
Taylor & Francis Group

X-Ray Studies of Two Liquid Crystalline Compounds

M. K. USHA,[1] N. VINUTHA,[1] R. SOMASHEKAR,[1] AND D. REVANNASIDDAIAH[2,*]

[1]Department of Studies in Physics, University of Mysore, Mysore, India
[2]PG Department of Physics, Saint Philomena's College (Autonomous), Mysore, India

X-ray studies of two liquid crystalline compounds, viz., p-ethoxybenzylidene p-heptylaniline (2O.7) and p-butoxybenzylidene p-heptylaniline (4O.7) are reported in this paper. The compound 2O.7 shows only a nematic phase while 4O.7 exhibits SmB, SmC, SmA, and nematic phases. Using powder X-ray diffraction patterns recorded at different temperatures, the microstructural parameters, and pair correlation function of these compounds have been estimated. The results obtained are inferred in terms of molecular ordering present in their nematic and smectic phases.

Keywords Liquid crystals; microstructural parameters; 2O.7; 4O.7; pair correlation function; X-ray diffraction

1. Introduction

X-ray diffraction (XRD) is one of the most useful techniques to probe the structures of a wide range of materials [1]. In the case of liquid crystals, XRD technique is effectively employed to extract information about the nature and degree of ordering present in different liquid crystalline phases. Further, XRD technique is often used for phase identification of liquid crystalline materials and to estimate layer thickness and interplanar spacing in smectic phases [1–4]. In the powder XRD profiles of liquid crystals, the maxima at the smaller angle are related to the length of the molecule while those at the larger angle are due to interaction of neighboring, parallel molecules. These reflections can be used to estimate respectively, the molecular length/layer thickness (d_1) and intermolecular/interplanar spacing (d_2) [1].

Nematics have long-range orientational order while smectics exhibit additional short-range positional order and short/long-range bond orientational order. In liquid crystalline phases, the order is confined to microscopic/macroscopic domains. The finite size of these domains (crystallite size or domain size) and microstrains give rise to volume defects, which affect the intensity of the diffracted X-ray peaks. To be precise, the crystallite size is the number of smectic/nematic layers times the thickness of the layers in a direction perpendicular to the plane of the layers and it is measured in Angstrom while microstrain

*Address correspondence to Dr. D. Revannasiddaiah, PG Department of Physics, Saint Philomena's College (Autonomous), Mysore Bangalore Road, Bannimantap, Mysore 570015, Karnataka, India. E-mail: dr@physics.uni-mysore.ac.in

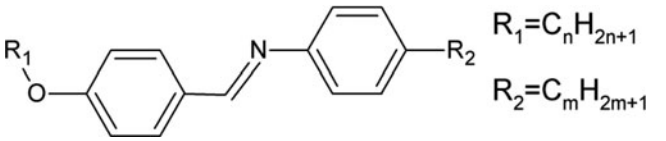

Figure 1. General molecular structure of nO.m compounds.

results from displacement of atoms from their mean positions due to dislocations, composition fluctuations, etc. These defects can be quantitatively analyzed by employing line profile analysis method [5, 6].

Correlations in atomic/molecular positions can be quantitatively expressed by defining the pair correlation function (PCF). Estimation of PCF of a system gives information about the nature of molecular ordering present in the system. PCF can be calculated by Fourier transformation of the total structure factor obtained from neutron and XRD experiments [7–9].

In the present work, microstructural parameters (viz., crystallite size/domain size and microstrain) and PCF studies of two liquid crystalline compounds, viz., p-ethoxybenzylidene p-heptylaniline (2O.7) and p-butoxybenzylidene p-heptylaniline (4O.7) are reported using XRD technique. These compounds belong to the class of N-(p-n-alkoxybenzylidene)-p-n-alkylanilines, popularly known as the Schiff's base nO.m compounds (where *n* and *m* denote the alkyl chain lengths on either side of the rigid core). The general molecular structure of nO.m compounds is shown in Fig. 1. Since their first synthesis in 1969 [10] till date, the complex but subtle polymorphism exhibited by these compounds has motivated several investigators to use them for the study of fundamental aspects of liquid crystals [11–17]. The calorimetric [12], X-ray studies [13], NMR [14], refractive index, and density measurements [15] of the compound 4O.7 have been reported in literature. Smith et al. [16] have reported the calorimetric and texture studies of 2O.7. Pandey et al. [17] have studied the effects of doping polymer poly(isobutylmethacrylate) on the dielectric and electro-optical parameters of 2O.7.

2. Theory

2.1. Microstructural Parameters

In case wherein one peak is present in the X-ray intensity profile of the sample, then, crystallite size (D) can be estimated using the Debye–Scherrer's equation [18]:

$$D = \frac{K\lambda}{\beta \cos\theta} \tag{1}$$

and microstrain (ε) can be estimated using the equation [19]:

$$\varepsilon = \frac{\beta}{4\tan\theta}. \tag{2}$$

Here, β is the integral breadth of the XRD peak (i.e., full width at half maximum), λ is the wavelength of the incident X-rays, θ is the Bragg angle and K is the shape factor which is usually taken as unity.

In case there is more than one peak present in the X-ray intensity profile, then, crystallite size and microstrain can be computed using the Williamson-Hall equation [20]:

$$\frac{\beta \cos\theta}{\lambda} = \frac{1}{D} + \varepsilon.\frac{4\sin\theta}{\lambda} \tag{3}$$

A plot of $(\beta\ \cos\theta)/\lambda$ against $(4\ \sin\theta)/\lambda$ (Williamson–Hall plot) gives a straight line with a y-intercept equal to the inverse of crystallite size and slope equal to the value of microstrain.

2.2. Pair Correlation Function

The total structure factor, $S(Q)$ (which is proportional to the intensity $I(Q)$ of the incident X-rays) can be obtained from XRD experiment. Then, PCF can be calculated by Fourier transformation of $S(Q)$ using the expression:

$$g(r) = 1 + \frac{1}{2\pi\, r\rho_o}\int_0^\infty Q[S(Q) - 1]\sin(Qr)\mathrm{d}Q \tag{4}$$

where Q is the scattering vector, r is the inter molecular distance, and ρ_0 is the average density of the system comprising N particles [7–9]. This particular study gives variation in the molecular arrangements in the neighborhood of the molecules at different temperatures and in different phases.

3. Experimental

The samples 2O.7 and 4O.7 were obtained from M/s Frinton Laboratories Inc., USA (purity 99%) and used without further purification. The transition temperatures (in °C) exhibited by the compounds as determined using polarizing microscope and DSC are as given below:

2O.7: (Cr) 54.49 (N) 86.76 (I)
4O.7: (SmB) 45.9 (SmC) 47 (SmA) 54 (N) 80.8 (I)

with Cr, N, I, and Sm denoting crystal, nematic, isotropic, and smectic phases, respectively.

Powder XRD patterns were recorded using PANalytical Empyrean X-ray diffractometer (Model No. DY1042) and a PIXcel^{3D} detector with Cu$K\alpha$ radiation ($\lambda = 1.5406$ Å) at different temperatures. Representative X-ray profiles recorded in the nematic phase of 2O.7 and in the SmB, SmA and nematic phases of 4O.7 are shown in Fig. 2. No X-ray profiles were recorded in the SmC phase of the sample 4O.7 since its range is too narrow.

4. Results and Discussion

It is evident from Fig. 2 that the X-ray profile in the nematic phase of 2O.7 shows only one peak in the wide angle region where as the X-ray profile in the nematic phase of 4O.7 has an additional peak in the small angle region. This indicates that the nematic phase of 2O.7 is classical nematic and that of 4O.7 is cybotactic in nature [21]. The apparent molecular length/layer thickness (d_1) and interplanar/intermolecular spacing (d_2) and the microstructural parameters of 2O.7 and 4O.7 estimated to an accuracy of ±5% are given in Tables 1 and 2, respectively. Due to presence only wide angle peak in the X-ray profiles of 2O.7, only d_2 could be estimated, and crystallite size and microstrain have been estimated

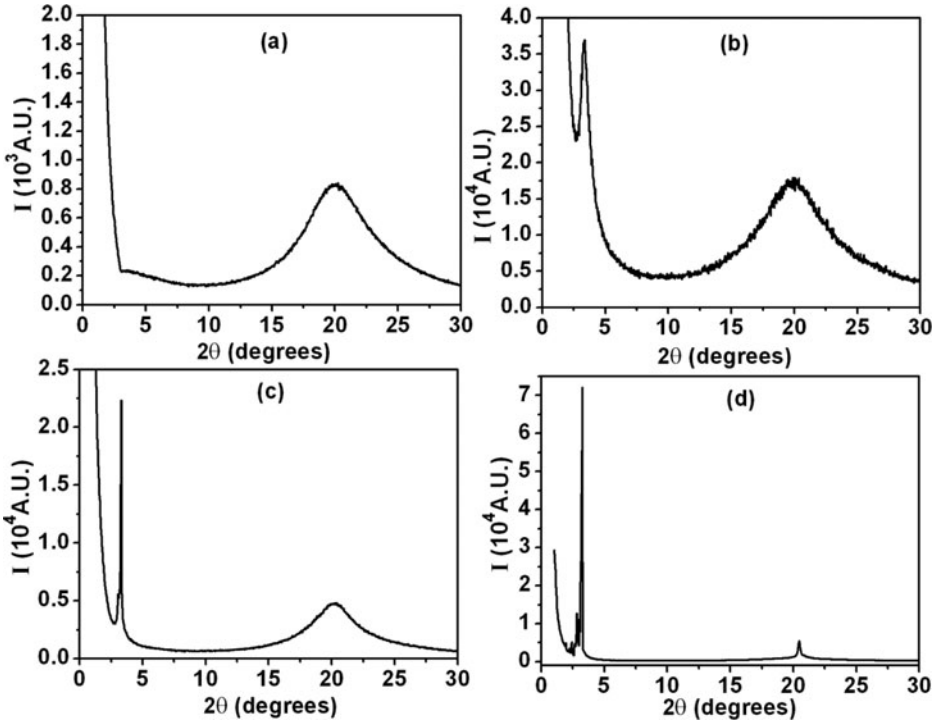

Figure 2. X-ray profiles recorded at (a) 71°C in the N phase of 2O.7; (b) 71°C in the N phase; (c) 51°C in the SmA phase; and (d) 42°C in the SmB phase of 4O.7.

employing equations (1) and (2), respectively. On the other hand, presence of both small angle and wide angle peak in the X-ray profiles of 4O.7 has enabled us to compute both d_1 and d_2, and crystallite size and microstrain in this case have been estimated employing equation (3). The trend in variation of d_1 and d_2 in different phases are in conformity with those reported in literature [22,23].

From Table 1, it is observed that in the case of 2O.7, the crystallite size has decreased with increase in temperature whereas microstrain has increased. This is in accordance with our expectation because with increase in temperature, the ordering of the molecules is disturbed and hence, the crystallite size or domain size tends to decrease while the microstrain (resulting from displacement of atoms from their mean positions) increases. It

Table 1. Microstructural parameters in the nematic phase of 2O.7 at different temperatures

t (°C)	d_2 (Å)	D (Å)	ε ($\times 10^{-1}$)
55	4.39	16.60	1.192
63	4.41	16.04	1.238
71	4.42	15.64	1.274
79	4.44	15.17	1.317
85	4.45	14.81	1.353

Table 2. Microstructural parameters in different phases of 4O.7 at different temperatures

Phase	t (°C)	d_1 (Å)	d_2 (Å)	D (Å)	E_a (eV)	ε ($\times 10^{-2}$)
SmB	31	27.56	4.32	341.37	$(9.59 \pm 0.5) \times 10^{-3}$	0.216
	35	27.55	4.32	342.85		0.241
	39	27.48	4.33	344.24		0.289
	42	27.53	4.33	345.67		0.328
	45	27.61	4.34	346.93		0.384
SmA	49	26.91	4.39	281.43	$(7.90 \pm 0.4) \times 10^{-2}$	9.750
	50	26.91	4.39	285.70		9.806
	51	26.91	4.40	288.64		9.836
	52	26.90	4.40	289.20		9.892
	53	26.89	4.40	292.19		9.993
N	60	26.51	4.44	477.43	1.04 ± 0.05	11.27
	65	26.46	4.46	972.16		11.69
	70	26.41	4.47	1257.6		12.25
	74	26.40	4.48	2018.6		12.73
	79	26.28	4.49	3727.9		12.85

is also observed that the crystallite size obeys Arrhenius law:

$$D = D_0 \exp\left(-\frac{E_a}{k_B T}\right) \tag{5}$$

where, k_B is the Boltzmann constant and E_a is the activation energy for realignment of the molecules. The activation energy hence computed in the nematic phase of 2O.7 is found to be 0.037 eV.

It may be seen from Table 2 that in the case of 4O.7, both crystallite size and microstrain have increased with increase in temperature. This indicates that the domain size or in other words, molecular ordering is increasing with increase in temperature which is quite surprising. Moreover, activation energy, E_a is also found to be more in the nematic phase (1.04 eV) which occurs at higher temperature than in the smectic phases. This indicates that the thermal energy required for realignment is more in the nematic phase even though it is a more disordered system which is quite contrary to the expectation. This is due to the fact that 4O.7 being a long chain molecule, there is a tendency of unwinding of the chain at higher temperatures. The activation energy E_a in SmB phase (0.009 eV) is smaller than that in SmA phase (0.079 eV), which indicates that a little thermal energy is sufficient to nudge molecules to go over to SmA phase. Similarly, from SmA to nematic, a thermal energy of 0.079 eV is sufficient to dislodge the ordered SmA phase. Further, from nematic to isotropic, a thermal energy of 1.04 eV is sufficient to create isotropic order in the phase.

Figures 3 and 4 show the variation of PCF with inter molecular distance (r) at different temperatures in 2O.7 and 4O.7, respectively. From Fig. 3, it is observed that in 2O.7, the magnitude of PCF is low at the onset of nematic phase (55°C), increases as the nematic phase stabilizes (63°C) and then decreases near the N-I transition (79°C). In the case of 4O.7, there is a noticeable change in magnitude of PCF in different phases (Figure 4). The magnitude of PCF is highest in the SmA phase, lowest in the nematic phase and intermediate in the SmB phase. This is because the smectic phases are more ordered phases with higher

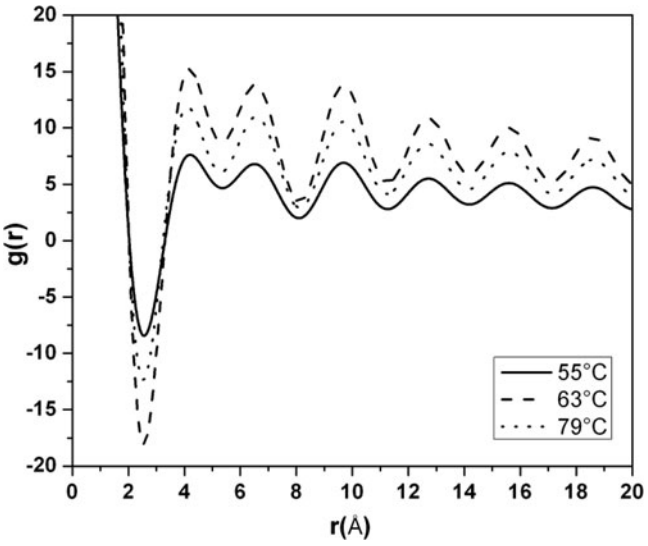

Figure 3. Variation of pair correlation function with intermolecular separation at different temperatures in the nematic phase of 2O.7.

PCF values compared to that of nematic phase. In the SmA phase, the molecules are in the most extended conformation [24], thereby, increasing the pair correlations, whereas, they are closely packed in the SmB phase. It is significant to note that, the SmA phase occurs at higher temperature than the SmB phase. Hence, in this particular case, we have higher PCF values in the SmA phase. In both 2O.7 and 4O.7, the peaks in the PCF are observed at the

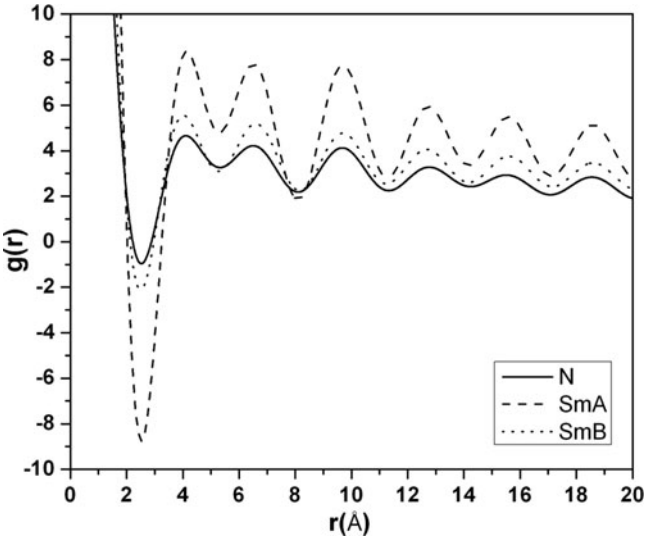

Figure 4. Variation of pair correlation function with intermolecular separation in different phases of 4O.7 (at selected temperatures).

r values of about 4.2, 6.5, 9.7, 12.7, 15.6, and 18.6 Å and they correspond to the distances of nearest neighboring molecules [8].

In conclusion, for the first time, we are reporting the microstructural parameters (viz., crystallite/domain size and microstrain) and PCF studies of liquid crystalline materials. In the case of 2O.7, crystallite/domain size is observed to decrease with increase in temperature whereas microstrain increases which is in accordance with our expectations. But in the case of 4O.7, both crystallite size and microstrain are found to increase with increase in temperature. The former observation is due to the fact that the molecular arrangement becomes more ordered with increase in temperature resulting in increased domain size. It is observed that PCF attains different magnitudes in different liquid crystalline phases. This indicates that the magnitude of PCF provides an insight into the molecular ordering present in individual phases. We have also quantified thermal energies required for a change over from SmB→SmA; SmA→N and N→I phases.

Acknowledgments

Authors acknowledge Dr. R. Pratibha, Mrs. Deepa Bhat, and Mrs. K. N. Vasudha, Raman Research Institute (RRI), Bangalore, for their assistance in the collection of X-ray data. Author M.K.U. acknowledges the Department of Science and Technology (DST), New Delhi for the award of INSPIRE fellowship. N.V. is grateful to the University Grants Commission (UGC), New Delhi for the award of RFSMS fellowship. D.R. is thankful to the UGC for financial support under Major Research Project Scheme [F.No.41-882/2012 (SR)]. Authors R.S. and D.R. acknowledge UGC, New Delhi for funding under UPE project.

References

[1] Azároff, L. V. (1980). *Mol. Cryst. Liq. Cryst.*, *60*, 73.
[2] Ghosh, S., Mandal, P., Paul, S., Paul, R. & Neubert, M. E. (2001). *Mol. Cryst. Liq. Cryst.*, *365*, 703.
[3] Urban, S., Przedmojski, J. & Czub, J. (2005). *Liq. Cryst.*, *32*, 619.
[4] Das, M. K., Roy, P. D., Paul, S. & Das, B. (2006). *Mol. Cryst. Liq. Cryst.*, *457*, 55.
[5] Guinebreitière, R. (2007). *X-ray Diffraction by Polycrystalline Materials*. Wiley-ISTE Ltd.: London, UK.
[6] Snyder, R. L., Fiala, J. & Bunge, H. J. (Eds.). (1999). *Defect and Microstructure Analysis by Diffraction: IUCr Monographs on Crystallography, No. 10*. Oxford University Press: Oxford, UK.
[7] Frenkel, D. & Smit, B. (1996). *Understanding Molecular Simulation: From Algorithms to Applications*. Academic Press: San Diego, USA.
[8] Egami, T. & Billinge, S. J. L. (2003). *Underneath the Bragg Peaks: Structural Analysis of Complex Materials*. Elsevier: Amsterdam, Netherlands.
[9] Lin, Z. & Zhigilei, L. V. (2006). *Phys. Rev. B*, *73*, 184113.
[10] Kelker, H. & Scheurle, B. (1969). *Angew. Chem. Int. Edn. 8*, 884.
[11] Rananavare, S. B. & Pisipati, V. G. K. M. (2011). *Liquid Crystalline Organic Compounds and Polymers as Materials of the XXI Century: From Synthesis to Applications*, Iwan, A. & Balcerzak E. S. (Eds.), Chapter 2, Transworld Research Network: Trivandrum, India.
[12] Bloemen, E. & Garland, C. W. (1981). *J. Phys. France*, *42*, 1299.
[13] Garland, C. W., Meichle, M., Ocko, B. M., Kortan, A. R., Safinya, C. R., Yu, L. J., Litster, J. D. & Birgeneau, R. J. (1983). *Phys. Rev. A*, *27*, 3234.
[14] Ravindranath, G., Venu, K. & Sastry, V. S. S. (1990). *Chem. Phys.*, *140*, 299.
[15] Rao, N. V. S., Potukuchi, D. M. & Pisipati, V. G. K. M. (1991). *Mol. Cryst. Liq. Cryst.*, *196*, 71.

[16] Smith, G. W., Gardlund, Z. G. & Curtis, R. J. (1973). *Mol. Cryst. Liq. Cryst.*, *19*, 327.
[17] Pandey, S., Gupta, S. K., Singh, D. P., Vimal, T., Tripathi, P. K., Srivastava, A. & Manohar, R. (2014). *Polym. Eng. Sci.*, doi:10.1002/pen.23907.
[18] Scherrer, P. (1918). *Nachr. Ges. Wiss. Göttingen.*, *26*, 98. [German].
[19] Mote, V. D., Purushotham, Y. & Dole, B. N. (2012). *J. Theor. Appl. Phys.*, *6*, 1.
[20] Williamson, G. K. & Hall, W. H. (1953). *Acta Metall.*, *1*, 22.
[21] de Vries, A. (1970). *Mol. Cryst. Liq. Cryst.*, *10*, 219.
[22] Lobo, C. V., Krishna Prasad, S., & Shankar Rao, D. S. (2004). *Phys. Rev. E*, *69*, 051706.
[23] Juszyńska, E., Jasiurkowska, M., Arodź, M. M., Takajo, D. & Inaba A. (2011). *Mol. Cryst. Liq. Cryst.*, *540*, 127.
[24] de Vries, A. (1973). *Mol. Cryst. Liq. Cryst.*, *20*, 119.